

# Biomechanical Analysis of Maxillary Expansion in CLP Patients

Christof Holberg<sup>a</sup>; Nikola Holberg<sup>b</sup>; Katja Schwenzer<sup>c</sup>; Andrea Wichelhaus<sup>d</sup>; Ingrid Rudzki-Janson<sup>e</sup>

## ABSTRACT

**Objective:** To carry out a comparative biomechanical analysis of maxillary low force expansion using the quadhelix appliance in cleft and noncleft patients. We also intended to determine whether a sufficient transverse skeletal effect could be achieved among cleft patients using the quadhelix appliance.

**Materials and Methods:** Three finite element models of the viscerocranium and neurocranium were established in which a transverse expansion of the maxilla using a quadhelix (transverse force of 2 N) was simulated.

**Results:** The skeletal effects at the anatomic structures of the midface and the cranial base were far more marked in the simulation models with clefts compared to the morphologically normal state. The highest expansions were measured for bilateral cleft palates. Thus, the expansion measured at the supraorbital margin was 4.7  $\mu$ strain with a bilateral cleft, 2.1  $\mu$ strain with a unilateral cleft, and only 0.2  $\mu$ strain with the morphologically normal state. For bilateral and also for unilateral bone clefts, the skeletal effect of a maxillary low force expansion with a quadhelix on the anatomical structures of the viscerocranium and neurocranium is very much larger than is the case for individuals without clefts.

**Conclusion:** In the presence of a continuous cleft in the jaw and palate area, orthodontic forces (quadhelix) are apparently already sufficient to allow a skeletal expansion of the maxilla. Maxillary expansion using the quadhelix appliance represents a reasonable alternative to using conventional rapid maxillary expansion appliances among cleft patients.

**KEY WORDS:** Maxillary expansion; Cleft lip and palate; Quadhelix; Finite element method

## INTRODUCTION

The objective of a maxillary expansion is to bring about a transverse skeletal expansion of the maxilla,<sup>1</sup> while avoiding any dental side effects wherever possible.<sup>2</sup>

In order to achieve this skeletal effect, the use of a stable maxillary expansion appliance is necessary for patients who do not suffer from clefts in the jaw and palate area.<sup>1,3</sup> This special equipment should be able to produce high forces of up to 120 N<sup>4-7</sup> in order to create an opening of the median palatal suture and a lateral bending of the maxillary structures. Unlike the situation with noncleft individuals, skeletal stability in the transverse direction is reduced<sup>8</sup> in cleft palate patients because of the special anatomical situation in the jaw and palate area, which can even lead occasionally to a collapse of lateral segments in the medial direction.<sup>8-12</sup>

With cleft palate patients, an indication for a transverse maxillary expansion often exists because the maxilla is excessively narrow.<sup>8,10-13</sup> Unlike noncleft patients, the necessary skeletal widening of the maxilla with cleft patients is not carried out, according to some authors, using a conventional rapid maxillary expansion appliance, but rather using a quadhelix appara-

<sup>a</sup> Postdoc, Department of Orthodontics, University of Munich, Munich, Bavaria, Germany.

<sup>b</sup> Research Scientist, Department of Orthodontics, University of Munich, Munich, Bavaria, Germany.

<sup>c</sup> Postdoc, Department of Maxillofacial Surgery, University of Basel, Basel, Switzerland.

<sup>d</sup> Professor and Department Chair, Department of Orthodontics and Pediatric Dentistry, University of Basel, Basel, Switzerland.

<sup>e</sup> Professor and Department Chair, Department of Orthodontics, University of Munich, Munich, Bavaria, Germany.

Corresponding author: Dr Christof Holberg, Department of Orthodontics, University of Munich, Goethestrasse 70, Munich, Bavaria 80336, Germany (e-mail: christof.holberg@med.uni-muenchen.)

Accepted: May 2006. Submitted: April 2006.

© 2007 by The EH Angle Education and Research Foundation, Inc.

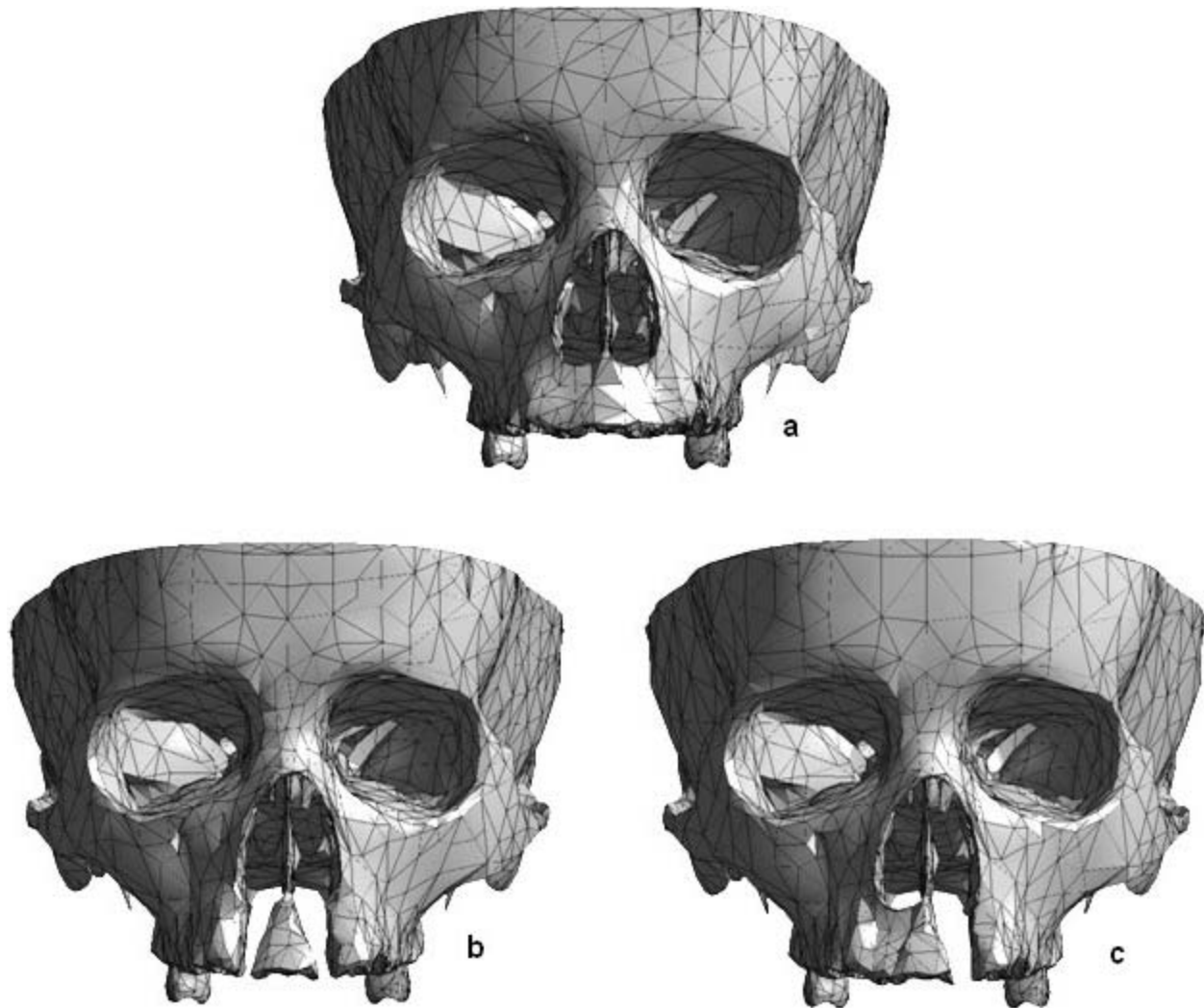


**Figure 1.** Finite element model (a) without a bone cleft, (b) with a bilateral bone cleft, and (c) with a unilateral left-sided bone cleft.

tus<sup>10-13</sup> that is only able to generate orthodontic<sup>14</sup> transverse forces up to 5 N. According to Reitan,<sup>14</sup> forces in this area are well able to induce a dental effect, but for a skeletal effect, higher orthopedic forces<sup>14</sup> that should be greater than 5 N are required. Biomechanical studies on the special anatomical situation with cleft patients have not been published in the literature up until now, and expansions induced by quadhelix therapy in the skeletal structures of the viscerocranium and neurocranium also remain unexplained.

The goal of the present study was therefore to carry out a comparative biomechanical analysis of maxillary low force expansion and quadhelix apparatus-induced expansion among cleft and noncleft individuals using a finite element method (FEM). Another goal was to clarify how effective the skeletal effect of the quadhelix appliance is among patients with a cleft jaw and palate and whether the quadhelix appliance represents a rea-

sonable alternative to using conventional rapid maxillary expansion equipment among cleft patients.

## MATERIALS AND METHODS

For carrying out comparative simulations, three finite element models of the viscerocranium and neurocranium were generated (Figure 1). The first simulation model revealed no clefts in the jaw or palate area, the second featured a bilateral cleft, and the third featured a unilateral cleft formation on the left side (Figure 1).

All three finite elements models were derived from the skull of a 20-year-old male adult that was available as a precise anatomic plastic model (Somso, Coburg, Germany). The surface of this anatomic skull model was digitalized using a three-dimensional scanner supplied by Minolta (Langenhagen, Germany), cleaned of irregular surfaces using Rapidform<sup>™</sup> software (Inus Technology Inc, Seoul, South Korea),

**Table 1.** Properties of Experimental Parameters

Parameter	Conditions in Study
Young's modulus juvenile skull	13.7 GPa
Young's modulus teeth	22.0 GPa
Poisson's ratio	0.3
No. of elements (mean)	30,910
Bilateral cleft	29,889
Unilateral cleft	30,138
No cleft	32,702
No. of nodes (mean)	56,435
Bilateral cleft	55,016
Unilateral cleft	55,064
No cleft	59,226
Zero-displacement	Nodes at the rear edge of foramen magnum
Area of force application	Palatal side of first upper molar crowns (0.5 cm <sup>2</sup> each side)
Level of force	2 N each side

matched, smoothed, and then transferred into a virtual computer aided design (CAD) model consisting of bilinear non-uniform rational B-spline (NURBS) patches. The course of the bony clefts was modeled afterwards in the area of the jaw and the palate interactively, just as the inner part of the maxillary sinus was.

For applying the transversely acting forces of the quadhelix, the first upper molars were considered in the simulation model (Figure 1). The anatomic model variants generated by this procedure were imported into Design Space™ (Ansys Inc, Canonsburg, Pa) software, where they were cross-linked three-dimensionally to form a finite element model, only with parabolic tetrahedral elements being employed. The topology of element SOLID 187 was tetrahedral, with 4 nodes at each corner, 6 lines between the corners, and 6 nodes that halved each line, so each tetrahedral element consisted of 10 nodes. SOLID 187 had a quadratic displacement behavior and was well suited to modeling irregular meshes. The simulations could then be carried out after assignment of the material properties and thresholds (Table 1).

For all comparative calculations, an orthodontic transverse force of 2 N was applied to each palatal side of the first upper molars, which corresponded to the force delivered by a moderately activated quadhelix apparatus. Except for the anatomical cleft form, all experimental conditions were kept constant with all calculations (Table 1). After completion of the calculations, the comparative expansions appearing (in  $\mu$ strain) were recorded in tabular form and the relationships between the expansions for the individual cleft forms were visualized in diagrammatic form with Design Space software using an interactive tool at previously defined anatomical points of the midface and cranial base (Table 2). The distribution of the expansions above the anatomical structures of the viscerocranium and neurocranium could be represented in all three dimensions using false-color coding (Figures 2

through 4) and comparably with one another for the individual cleft forms.

## RESULTS

The smallest expansions for all the measurement points in the midface were measured with the simulation model featuring no cleft. The differences in measurements between the cleft and noncleft models were almost considerable (Table 2). At the nasofrontal suture, the measured expansion in the noncleft model was 0.3  $\mu$ strain (Figures 2 and 5), whereas in the model with bilateral cleft formation the value at 8.2  $\mu$ strain was 27-fold higher (Figures 3 and 5). For the simulation model with a unilateral cleft, the measured expansions (Figures 4 and 5) at the nasofrontal suture were 4.0  $\mu$ strain (cleft side) and 3.7  $\mu$ strain (healthy side). At the supraorbital margin (Figure 6) the expansion in the simulation model without cleft formation was 0.2  $\mu$ strain, whereas in the models with cleft formation it was 4.7  $\mu$ strain (bilateral), 2.1  $\mu$ strain (unilateral, cleft side) and 2.1  $\mu$ strain (unilateral, healthy side).

However, at the measurement points in the infraorbital margin and the zygomaticoalveolar crest, the differences between cleft and noncleft models were clearly smaller (Figure 5). Thus, at the zygomaticoalveolar crest in the finite element model without cleft formation, 5.2  $\mu$ strain was measured, whereas for the model with a bilateral cleft the measurement was 7.6  $\mu$ strain, and with the unilateral cleft it was 7.0  $\mu$ strain (cleft side) and 6.4  $\mu$ strain (healthy side). The differences at the zygomaticofrontal suture between the noncleft and the cleft models, however, were once again distinct. The highest expansions in the midface were always registered in the simulation model with bilateral cleft jaw and palate (Table 2). In the unilateral cleft model, however, expansions were lower than those measured with the bilateral cleft (Table 2), but usually higher than those in the model without cleft

**Table 2.** Measured Strains at the Anatomical Structures of the Midface and the Cranial Base in Simulation Models With a Bilateral Cleft, a Unilateral Cleft, and No Cleft

Anatomical Structure	Strain ( $\mu$ strain)			
	No Cleft	Bilateral Cleft	Unilateral Cleft (Cleft Side)	Unilateral Cleft (Normal Side)
Zygomatic bone	1.0	2.6	2.4	1.9
Zygomaticoalveolar crest	5.2	7.6	7.0	6.4
Zygomaticofrontal suture	2.3	8.1	6.3	5.1
Infraorbital foramen	2.2	2.5	1.7	1.6
Infraorbital margin	2.5	3.6	2.7	2.4
Anterior wall of maxillary sinus	1.9	1.1	1.1	0.7
Nasofrontal suture	0.3	8.2	4.0	3.7
Supraorbital margin	0.2	4.7	2.1	2.1
Pterygopalatal fossa	0.6	3.4	3.2	2.9
Medial lamina of pterygoid	0.5	6.9	1.4	1.0
Pterygoid fossa	0.8	5.3	5.2	4.1
Lateral lamina of pterygoid	0.7	9.6	1.9	1.3
Optic foramen	0.7	3.8	8.2	6.8
Superior orbital fissure	0.5	4.7	5.7	4.4
Spinous foramen	0.2	0.9	0.8	0.8
Oval foramen	0.3	3.7	3.3	3.2
Lacerated foramen	0.4	3.5	2.6	2.4
Round foramen	0.4	2.8	3.0	2.2
Internal auditory canal	0.1	1.3	0.9	0.9
Frontal crest	0.4	3.6	2.9	2.9
Cribrosal lamina	0.8	6.7	6.1	6.1
Orbital part of frontal bones	0.2	1.3	1.1	1.2
Pituitary fossa	0.4	3.5	2.9	2.9
Carotid sulcus	0.5	3.0	3.6	3.2
Spheno-occipital synchondrosis	0.1	0.6	0.7	0.7
Petrosal part of temporal bone	0.1	0.9	0.8	0.7
Squamosal part of temporal bone	0.1	2.0	1.7	1.6
Jugular foramen	0.1	1.2	0.9	0.8

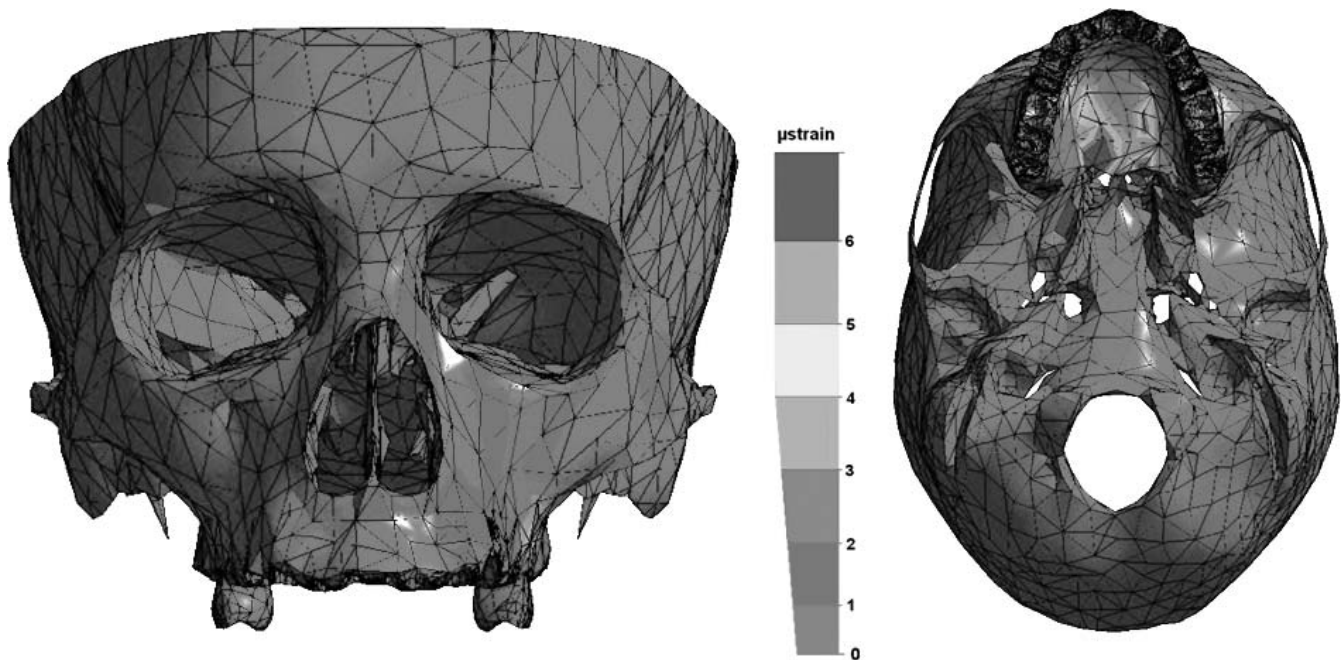


**Figure 2.** Level and distribution of the measured expansions after a 2-N transverse loading of the simulation model without a bone cleft.



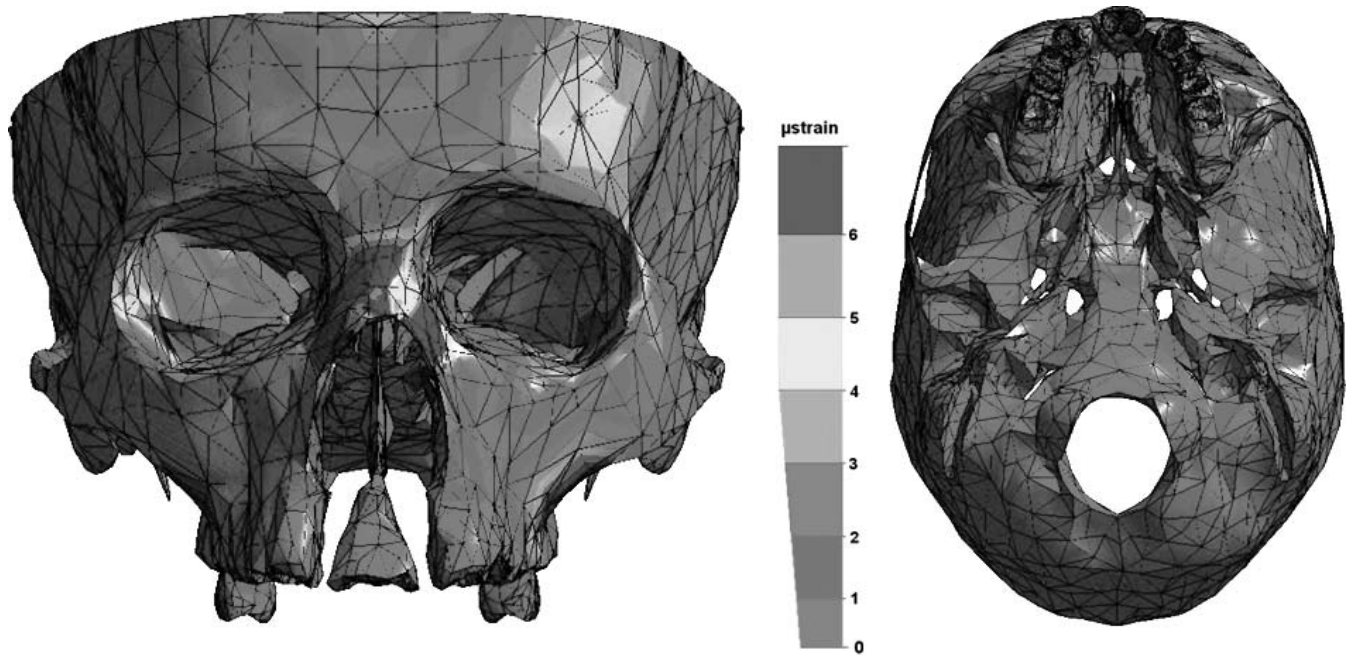


**Figure 3.** Level and distribution of the measured expansions after a 2-N transverse loading of the simulation model with a bilateral bone cleft.

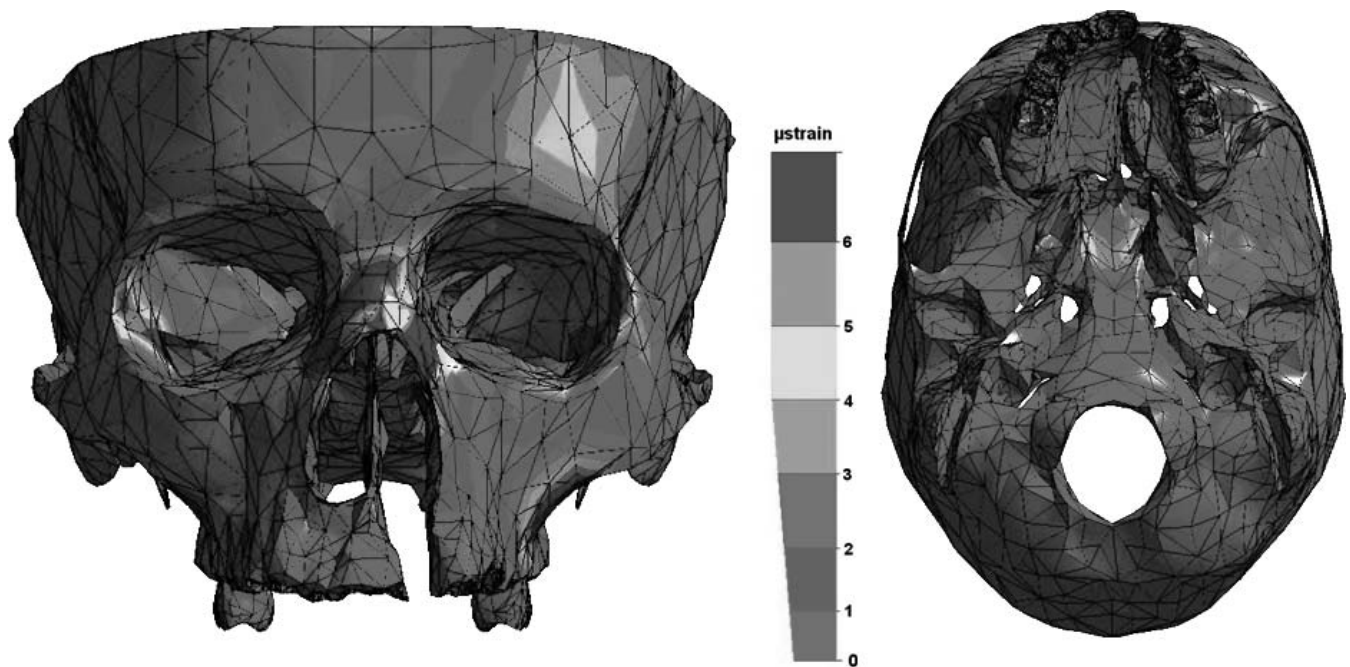


**Figure 4.** Level and distribution of the measured expansions after a 2-N transverse loading of the simulation model with a left-sided unilateral bone cleft.

formation. In the simulation model with the left-sided cleft, there were usually slightly higher expansions on the cleft side than was the case on the side that was not clefted (Figure 5). The picture with the anatomical structures of the cranial base was similar to that seen with the midface. Here as well, the lowest expansions were measured in the simulation model without cleft-

ing (Table 2; Figure 6). Examples included the optic foramen, the superior orbital fissure, and the oval foramen (Figures 2 and 6). Unlike the midface, the maximum values at the structures of the cranial base occurred both with the bilateral cleft model and with the unilateral cleft model (Figure 6). For almost all measurement points at the cranial base, the expansion on

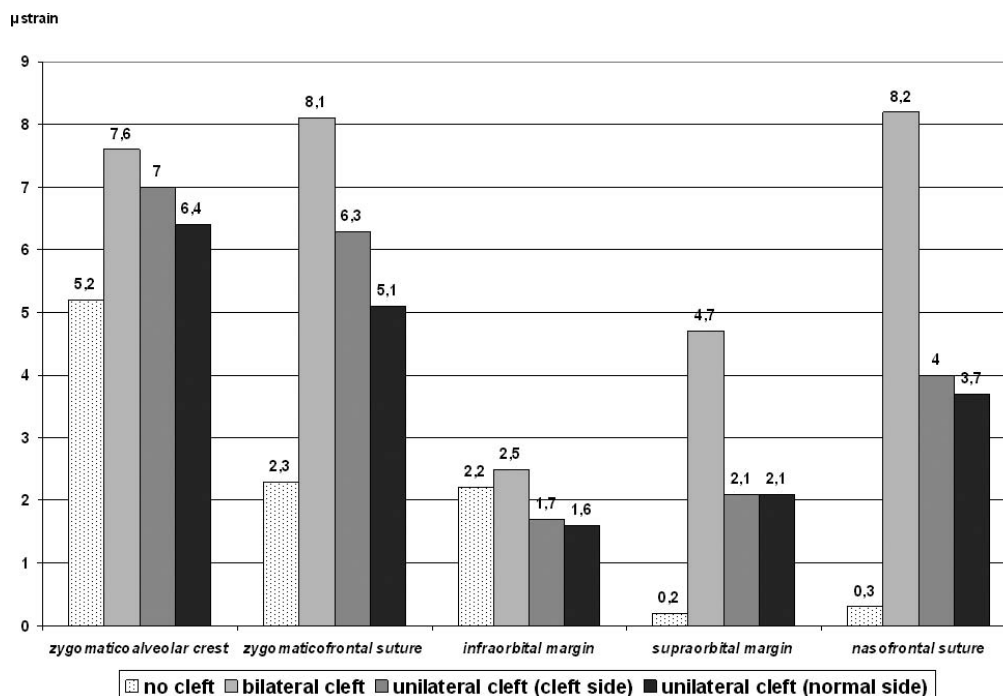


**Figure 5.** Expansions measured at different structures of the midface with simulation of maxillary expansion without a bone cleft, with a bilateral bone cleft, and with a unilateral bone cleft.

the cleft side was only slightly higher than the value measured on the nonaffected side (Table 2; Figure 6).

**DISCUSSION**

The FEM is a well-proven mathematical instrument for studying orthodontic problems.<sup>15-17</sup> The simulation models used in this case represent a simplified idealization of reality. The more differentiated and the more extensive the finite element model, the more precise and more realistic are the simulation results.

The geometric precision of depiction for the simulation models of the facial skull has been improved increasingly over the last years. Whereas in 1994 with Miyasaka-Hiraga et al<sup>18</sup> the finite elements model of the skull consisted of 1776 single elements, the model of Iseri et al<sup>16</sup> in 1998, which consisted of 2349 individual elements, was already more differentiated. The geometric precision increased further in the paper of Jafari et al<sup>17</sup> who introduced a simulation model of the skull with 6951 elements in 2003. Compared to the FEM models of the skull available up until now, the degree of anatomic differentiation was considerably improved in this paper, so that even finely-detailed anatomical structures, such as the foramina of the cranial base, could be considered in the mathematical model.

The simulation models of the facial skull and the cranial base used in the present paper consisted of approximately 30,000 individual elements with approximately 50,000 nodes (Table 1). Despite this relatively

differentiated illustration of the complex skull geometry, the present results allow only basic statements to be made about the different expansions upon transverse enlargement of the maxilla, because this still represents merely an artificial simulation model. Only simplified material properties that were based upon averaged values and taken from the literature<sup>18-20</sup> were used.

Maxillary expansion using the quadhelix apparatus is usually carried out only in mixed dentition,<sup>10-12</sup> ie, at a time point when individual morphology greatly varies depending on the skeletal age of the patient.<sup>21</sup> In order to eliminate this age-dependent variability as a distorting factor in the simulations, all measurements were carried out in the present study on a simulation model of a 20-year-old adult, because the variability of the anatomical structures is smaller at this age than it is during the mixed dentition phase. The systematic error arising from this, however, must be considered when interpreting the results.

Future simulation studies should endeavor to compute the distribution of expansions for different individual and age-dependent anatomic states. The present simulations clearly showed that if a cleft jaw and palate are not present, the maxillary expansion with the quadhelix apparatus cannot achieve a relevant skeletal effect at the more remote structures of the midface and the cranial base (Table 2; Figures 5 and 6). One must therefore assume that this treatment is only locally ef-

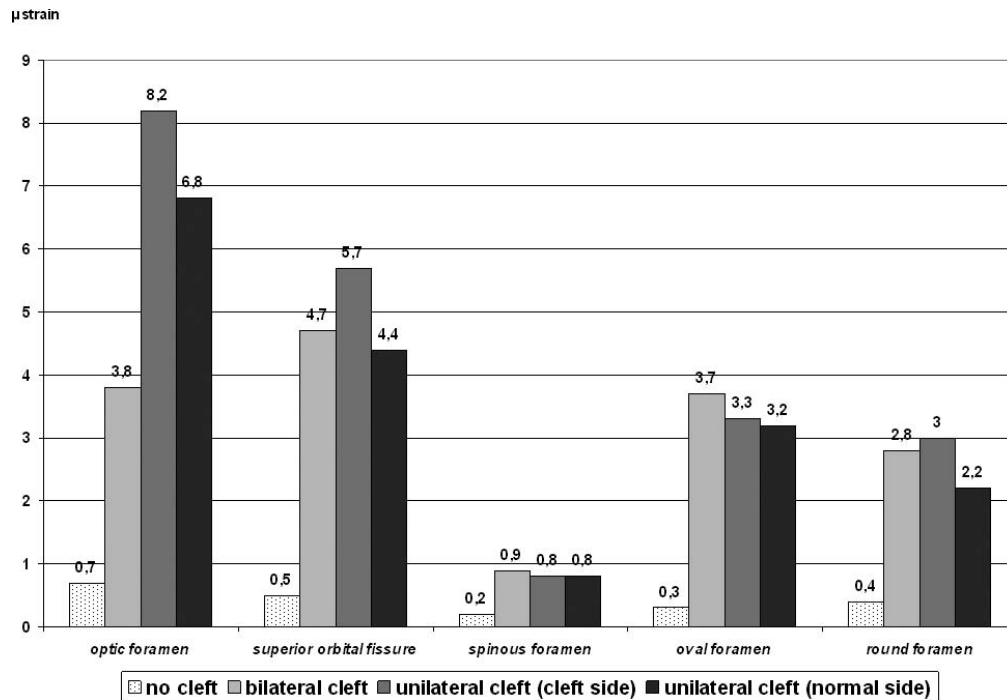


**Figure 6.** Expansions measured at different structures of the cranial base with simulation of maxillary expansion without a bone cleft, with a bilateral bone cleft, and with a unilateral bone cleft.

fective and leads only to a dental and not to a skeletal effect. However, the situation in which a cleft is present in the bone area of the jaw and hard palate is different. If orthodontic forces are applied using the quadhelix apparatus, skeletal effects do also arise at remote structures in the midface and the cranial base (Table 2; Figures 5 and 6). The calculations allow us to conclude that among patients with a unilateral or bilateral cleft, the use of a quadhelix appliance leads not only to a dental, but also to a skeletal effect.

The results reported here therefore represent an experimental confirmation of the clinical studies of Tindlund and Rygh<sup>10–12</sup> and Rygh and Tindlund.<sup>13</sup> Both authors were able to show the good clinical efficiency of the quadhelix apparatus in several papers studying maxillary expansion among cleft patients.<sup>10–13</sup> In place of the quadhelix appliance, our results suggest that other equipment can also be used to generate moderate transverse forces in cleft patients. Alternatives to the quadhelix apparatus include, for example, the compound palatal arch<sup>22</sup> and the modified maxillary expansion apparatus that only produces moderate forces upon activation of a special nickel-titanium expansion screw.<sup>23</sup> According to the present results, the use of a rapid maxillary expansion appliance with forces of 120 N<sup>4,5,7</sup> is not necessary among cleft patients because orthodontic forces of below 5 N already suffice to achieve a skeletal effect in the midface and the cranial base.

## CONCLUSIONS

- In the presence of a continuous cleft in the jaw and palate area, orthodontic forces (quadhelix) already suffice to bring about a skeletal widening of the maxilla.
- Maxillary expansion using the quadhelix appliance therefore represents a reasonable alternative to using conventional rapid maxillary expansion appliances among cleft patients.

## REFERENCES

1. Derichsweiler H. Die Gaumennahterweiterung. *Fortschr-Kieferorthop.* 1953;14:15.
2. Timms DJ. A study of basal movement with rapid maxillary expansion. *Am J Orthod.* 1980;77:500–507.
3. Chaconas SJ, Caputo AA. Observation of orthopedic force distribution produced by maxillary orthodontic appliances. *Am J Orthod.* 1982;82:492–501.
4. Isaacson RJ, Wood JL, Ingram AH. Forces produced by rapid maxillary expansion. Part I. Design of the force measuring system. *Angle Orthod.* 1964;34:256–260.
5. Isaacson RJ, Ingram AH. Forces produced by rapid maxillary expansion. Part II. Forces present during treatment. *Angle Orthod.* 1964;34:261–270.
6. Sander C, Hüffmeier S, Sander FM, Sander FG. Initial results regarding force exertion during rapid maxillary expansion in children. *J Orofac Orthop.* 2006;67:19–26.
7. Zimring JF, Isaacson RJ. Forces produced by rapid maxillary expansion. Part III. Forces present during retention. *Angle Orthod.* 1965;35:178–186.
8. Opitz C, Hochmuth M, Rabe H, et al. Unilateral cleft lip and

- palate. Relationship between morphology of the dentition and functional parameters of the tongue. *J Orofac Orthop.* 1997;58:270–281.
9. Hawley CA. A study of maxillary movement. *Dent Items Interest.* 1912;34:426–451.
  10. Tindlund RS, Rygh P, Boe OE. Intercanine widening and sagittal effect of maxillary transverse expansion in patients with cleft lip and palate during the deciduous and mixed dentitions. *Cleft Palate Craniofac J.* 1993;30:195–207.
  11. Tindlund RS, Rygh P. Maxillary protraction: different effects on facial morphology in unilateral and bilateral cleft lip and palate patients. *Cleft Palate Craniofac J.* 1993;30:208–221.
  12. Tindlund RS, Rygh P. Soft-tissue profile changes during widening and protraction of the maxilla in patients with cleft lip and palate compared with normal growth and development. *Cleft Palate Craniofac J.* 1993;30:454–468.
  13. Rygh P, Tindlund R. Orthopedic expansion and protraction of the maxilla in cleft palate patients—a new treatment rationale. *Cleft Palate J.* 1982;19:104–112.
  14. Reitan K. The initial tissue reactions incident to orthodontic tooth movement are related to the influence of function. *Acta Odont Scand.* 1951;6:1–240.
  15. Holberg C. Effects of rapid maxillary expansion on the skull base—an FEM-analysis. *J Orofac Orthop.* 2005;66:54–66.
  16. Iseri H, Tekkaya AE, Oztan O, Bilgic S. Biomechanical effect of rapid maxillary expansion on the craniofacial skeleton, studied by the finite element method. *Eur J Orthod.* 1998;20:347–356.
  17. Jafari A, Shetty K, Kumar M. Study on stress distribution and displacement of various craniofacial structures following application of transverse orthopedic forces—a three-dimensional FEM study. *Angle Orthod.* 2003;73:12–20.
  18. Miyasaka-Hiraga J, Tanne K, Nakamura S. Finite element analysis for stresses in the craniofacial sutures produced by maxillary protraction forces applied at the upper canines. *Br J Orthod.* 1994;21:343–348.
  19. Tanne K, Hiraga J, Kakiuchi K, et al. Biomechanical effect of anteriorly directed extraoral forces on the craniofacial complex: a study using the finite element method. *Am J Orthod Dentofacial Orthop.* 1989;95:200–207.
  20. Tanne K, Hiraga J, Sakuda M. Effects of directions of maxillary protraction forces on biomechanical changes in craniofacial complex. *Eur J Orthod.* 1989;11:382–391.
  21. Enlow DH. *Principles of Bone Remodeling.* Springfield, Ill: Charles C Thomas; 1963.
  22. Wichelhaus A, Sander C, Sander FG. Development and biomechanical investigation of a new compound palatal arch. *J Orofac Orthop.* 2004;65:104–122.
  23. Wichelhaus A, Geserick M, Ball J. A new nickel titanium rapid maxillary expansion screw. *J Clin Orthod.* 2004;38:677–680.